

Why scaling up uncertain predictions to higher levels of organisation will underestimate change

James Orr*, Jeremy Piggott, Andrew Jackson, and Jean-François Arnoldi

*Zoology department, School of Natural Sciences,
Trinity College Dublin, The University of Dublin, Ireland.*

**jaorr@tcd.ie*

September 22, 2020

Abstract

Uncertainty is an irreducible part of predictive science, causing us to over- or underestimate the magnitude of change that a system of interest will face. In a reductionist approach, we may use predictions at the level of individual system components (e.g. species biomass), and combine them to generate predictions for system-level properties (e.g. ecosystem function). Here we show that this process of scaling up uncertain predictions to higher levels of organization has a surprising consequence: it will systematically underestimate the magnitude of system-level change, an effect whose significance grows with the system's dimensionality. This stems from a geometrical observation: in high dimensions there are more ways to be more different, than ways to be more similar. This general remark applies to any complex system. Here we will focus on ecosystems thus, on ecosystem-level predictions generated from the combination of predictions at the species-level. In this setting, ~~we show that higher~~the ecosystem's dimensionality is a measure of its ~~does not necessarily mean more constituent species, but more~~ diversity. ~~Furthermore, while~~ We explain why dimensional effects ~~can be obscured~~ do not play out when predicting change of a single linear aggregate property (e.g. total biomass), ~~they yet~~ are revealed when predicting change of non-linear ~~aggregate~~ properties (e.g. absolute biomass change, stability or diversity), and when several properties are considered at once to describe the ecosystem, as in multi-functional ecology. Our findings highlight ~~the~~ and describe the counter-intuitive ~~dimensional~~ effects of scaling up that inevitably play out when uncertain predictions, ~~are scaled up, and are therefore relevant to~~ effects that will occur in any field of science where a reductionist approach is used to generate predictions.

Keywords: Ecological Complexity, Diversity Metrics, Dimensionality, Mechanistic prediction, Multi-functionality, Multiple Stressors, Reductionism.

1 Introduction

In natural sciences, uncertainty of any given prediction is ubiquitous (Dovers & Handmer, 1992). When considering predictions of change, uncertainty has directional consequences: uncertain predictions will lead to either over- or underestimation of actual change. The reductionist approach to complex systems is to gather and use knowledge about individual components before scaling up predictions to the system-level (Levins & Lewontin, 1985; Wu, Jones, Li, & Loucks, 2006). Although scaling up to higher levels of organisation is general to the study of any complex systems, it is particularly well-defined in ecology. In this field, knowledge about the components at lower levels of organisation (individuals, populations) is commonly used to understand the systems at higher levels of organisation (communities, ecosystems) (Loreau, 2010; Woodward, Perkins, & Brown, 2010).

An unbiased prediction of an individual component is one that makes no systematic bias towards over- or underestimation for that component (Box 1). But what happens when we scale up unbiased predictions to higher levels of organisation? If we do not systematically underestimate the change of individual components, will this still be true when considering many components at once? When addressing this question, one must be wary of basic intuitions as the problem is inherently multi-dimensional, thus hard to properly visualize.

As a thought experiment, consider two ecological communities, one species-poor (low dimension) and the other species-rich (high-dimension). Both communities experience perturbations that change species biomass, and we assume that we have an unbiased prediction for this change, up to some level of uncertainty. We then scale up our predictions to the community-level, focusing on the change in Shannon's diversity index, caused by the perturbations. By comparing predicted and observed change we can quantify the degree of underestimation of our predictions, at the species and community-level. If we simulate this thought experiment (Fig. 1 and Appendix S4) we observe the following puzzling results, which motivate our subsequent analysis. Predictions of species biomass change may be unbiased (bottom row of Fig. 1), but when scaled up to the system level for the species-rich community, but not the species-poor community, we see a clear bias towards underestimation of change (top right corner of Fig. 1).

As we shall explain in depth, the reason for this emergent bias is that *in high dimensions there are more ways to be more different, than ways to be more similar* (Fig. 6a). Our goal is to make this statement quantitative and generally relevant to ecological problems. We start from a geometric approach showing that, in two dimensions, our claim can be visualised to reveal a positive relationship between magnitude of uncertainty and underestimation of change. Visualisation is only possible in low dimensions, but a more abstract reasoning demonstrates that as dimensionality increases so does the bias towards underestimation, which is further

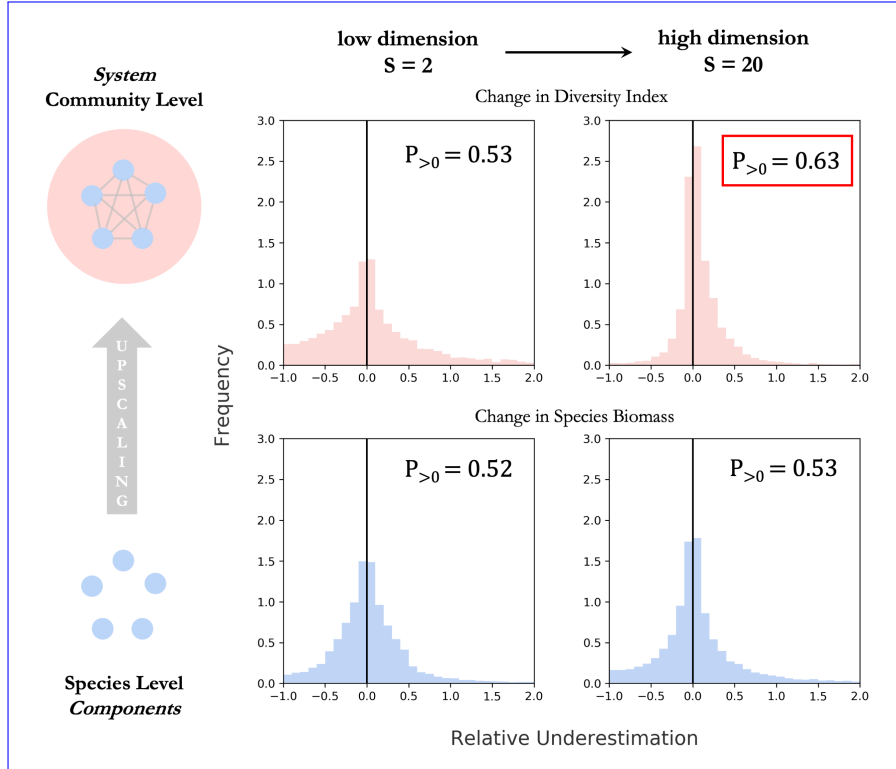


Figure 1: Simulated communities of 2 species (left) and 20 species (right) experienced 1000 perturbations (change in species biomass), for which we assume unbiased predictions at the species-level. Uncertainty around those predictions is simulated as a random terms of zero mean, independent across species. Histograms show the distribution of relative underestimation, defined as the difference between realized and predicted change expressed relatively to the predicted magnitude of change. By construction, there is no bias towards underestimation at the species level (bottom row). We then scale up our predictions to the community level to generate predictions for Shannon’s diversity index (top row). For the first, species poor community, this upscaling does not generate any bias. However, for the species rich community a bias emerges as approximately 75% of realizations show an underestimated magnitude of change. In this article, we explain in depth the statistical mechanisms behind this bias.

59 strengthened by larger uncertainty. We note that dimensionality is not necessarily an integer
 60 value. We propose that the effective dimensionality most relevant to ecological upscaling of
 61 predictions is not the number of species, but instead is a specific diversity metric, the Inverse
 62 Participation Ratio (IPR) (Wegner, 1980; Suweis, Grilli, Banavar, Allesina, & Maritan, 2015),
 63 comparable (but not equivalent) to Hill’s diversity indices (Hill, 1973).

64 We then explain why the effect of dimensionality depends on how change is measured at
 65 the system-level ([Fig. 6b Box 1](#)). If a single linear function is used to aggregate components
 66 (e.g. total biomass), dimensionality has no effect. An unbiased prediction for individual
 67 components trivially scales up to produce an unbiased system-level prediction. But this is not
 68 true in general. Non-linear functions (e.g. Shannon’s diversity index as in Fig. 1), can remain
 69 sensitive to dimensional effects. Predictions of change of these properties, even if constructed
 70 from unbiased predictions of individual components will be systematically underestimated.

71 The significance of this effect will depend on the relative significance of non-linearities in the
72 function of interest.

73 On simulated examples we will examine the behaviour of common ecosystem-level properties:
74 diversity, stability and total biomass. More generally, we emphasise that dimensional effects
75 will occur as soon as system-level change is measured as a change in multiple properties at once
76 (whether they are linear or not), as is the case in multi-functional descriptions of ecosystems
77 (Manning et al., 2018).

78 As a seemingly different kind of ecological case-study, we then revisit core questions of multiple-
79 stressor research in the light of our theory. In this field, there is a clear prediction (additivity
80 of stressor effects), a high prevalence of uncertainty about the the way stressors interact
81 (resulting in non-additivity) and, ultimately, great interest in the ecosystem-level consequences
82 of non-additive stressor interactions (synergism or antagonism) (Côté, Darling, & Brown, 2016;
83 Jackson, Loewen, Vinebrooke, & Chimimba, 2016; Piggott, Townsend, & Matthaei, 2015).
84 Expressed in this context, our theory predicts the generation of bias towards synergism when
85 multiple-stressor predictions are scaled up to higher levels of organisation.

86 Research has primarily focused on the causes of uncertainty, working hard to reduce it (Petchey
87 et al., 2015). Here we take a complementary approach by investigating the generic consequences
88 of uncertainty, regardless of the nature of the system studied or the underlying causes of
89 uncertainty. Our theory becomes more relevant as the degree of uncertainty increases, which
90 makes it particularly relevant for ecological problems. But, in fact, our findings could inform
91 any field of science that takes a reductionist approach in the study of complex systems (e.g.
92 economics, energy supply, demography, finance – see Box 2), demonstrating how dimensional
93 effects can play a critical role when scaling up predictions.

94 **2 Geometric Approach**

95 The central claim of this article is that *in high dimensions there are more ways to be more*
96 *different, than ways to be more similar*. We propose an implication: *a system-level predic-*
97 *tion based on unbiased predictions for individual components, will tend to underestimate the*
98 *magnitude of system-level change*.

99 To understand these statements, it is useful to take a geometrical approach to represent the
100 classic reductionist perspective, starting in two dimensions (Fig. 2a). Picture two intersecting
101 circles in a system's state-space (one blue, one red in Fig. 2). The first, blue circle is centred
102 on the system's initial state and its radius corresponds to the predicted magnitude of change.
103 The second, red circle is centred at the predicted state (which lies on the blue circle) and its

Box 1: Lexicon of Concepts

Reductionist view of complex systems

- *Components*: Individual variables B_i that together form a system (e.g. biomass of S species and abiotic compartments forming an ecosystem).
- *System state*: Point in *state space*, represented as a vector $\mathbf{B} = (B_1, \dots, B_S)$ jointly describing all system components.
- *Difference (or magnitude of change) between states*: the Euclidean distance $\|\mathbf{B} - \mathbf{B}'\|$ between two joint states \mathbf{B} and \mathbf{B}' .

Scaling up uncertain predictions

- *Relative error*: Magnitude of error caused by uncertainty relative to the magnitude of predicted change.
- *Aggregate system-level property*: Scalar function of the joint state (e.g. total biomass or diversity index)
 - *Linear aggregate property*: Linear function of joint state variables (e.g. total biomass).
 - *Non-linear property*: Non-linear function of joint state variables (e.g. diversity index).
- *Scaled up prediction*: A prediction made for the joint state, or a scalar property of the joint state, based on individual predictions for components.
- *Unbiased prediction*: A prediction that, despite uncertainties, does not systematically overestimate or underestimate the magnitude of change (of a joint state, a system component or an aggregate property).

Multi-functional view of complex systems

- Multivariate description of a complex system, based on multiple aggregate properties, or *functions* (production, diversity, respiration) instead of individual components (species biomass and abiotic compartments). The state of the system is the joint state $\mathbf{F} = (F_1, \dots, F_{S_F})$ of S_F functions. Difference between states is the distance between two joint functional states \mathbf{F} and \mathbf{F}' .

104 radius corresponds to the magnitude of realized error of the prediction, in other words, the
 105 realized outcome of the uncertainty associated with the prediction (red circle in Fig. 2). The
 106 actual final state is thus somewhere on that red circle. If it falls outside the blue circle, the
 107 prediction has underestimated the magnitude of change. The proportion of the red circle lying
 108 outside of the blue circle measures the proportion of possible configurations that will lead
 109 to an underestimation of change. In other words, for a given magnitude of error caused by
 110 uncertainty, this portion of the circle represents the states that are more different from the
 111 initial state than predicted. As the relative magnitude of error increases (as the red circle's
 112 diameter becomes larger, relative to that of the blue circle) this proportion grows (Fig. 2a).

113 In three dimensions these two intersecting circles become two intersecting spheres. The
 114 proportion of interest is the surface of the spherical cap lying outside of the sphere centred
 115 on the initial state. Here, a non-intuitive phenomenon occurs: with the same radii as in the
 116 2D case, in 3D there are now more configurations leading to underestimation. As dimensions
 117 increase this proportion increases, until the vast majority of possible states now lie in the
 118 domain where change is underestimated (Fig. 2b). This result can be made quantitative
 119 from known expressions for the surface of hyper-spherical caps. This gives us an analytical
 120 expression for the proportion of configurations leading to an underestimation of change, as a
 121 function of the relative magnitude of error (x) and dimension (S):

$$P_{>0}(x) = 1 - \frac{1}{2} I_{1-\frac{x^2}{4}} \left(\frac{S-1}{2}; \frac{1}{2} \right); \quad x = \frac{\|\text{error}\|}{\|\text{prediction}\|} \quad (1)$$

122 In the above equations $\|\cdot\|$ stands for the standard Euclidean norm of vectors¹, and $I_s(a, b)$ is
 123 the cumulative function of the β -distribution (Appendix S2). This is what we mean by *in high*
 124 *dimensions there are more ways to be more different, than ways to be more similar*. To see how
 125 this relates to the scaling up of unbiased predictions of individual components ([Box 1](#)), we now
 126 take a statistical approach. Suppose we uniformly sample the intersecting circles, spheres and
 127 hyper-spheres defined above and drawn in Fig. 2. The proportion Eq. (1) becomes a probability,
 128 the probability of having underestimated change. This uniform sampling is precisely what
 129 happens if the uncertainty of individual variables ~~acts as~~ are independent random normal
 130 variables with zero mean ([a particular case of an](#) unbiased uncertainty at the component level,
 131 see Appendix S2). This justifies our second claim: *a system-level prediction based on unbiased*
 132 *predictions for individual components, will tend to underestimate the magnitude of change of*
 133 *the system state*.

134 This reasoning is geometrical, and relies on a computation of the surface of classic shapes such
 135 as hyper-spheres and spherical caps. But the core mechanism behind the behaviour of the

¹This is the most convenient norm for our geometrical approach but other norms would give similar results.

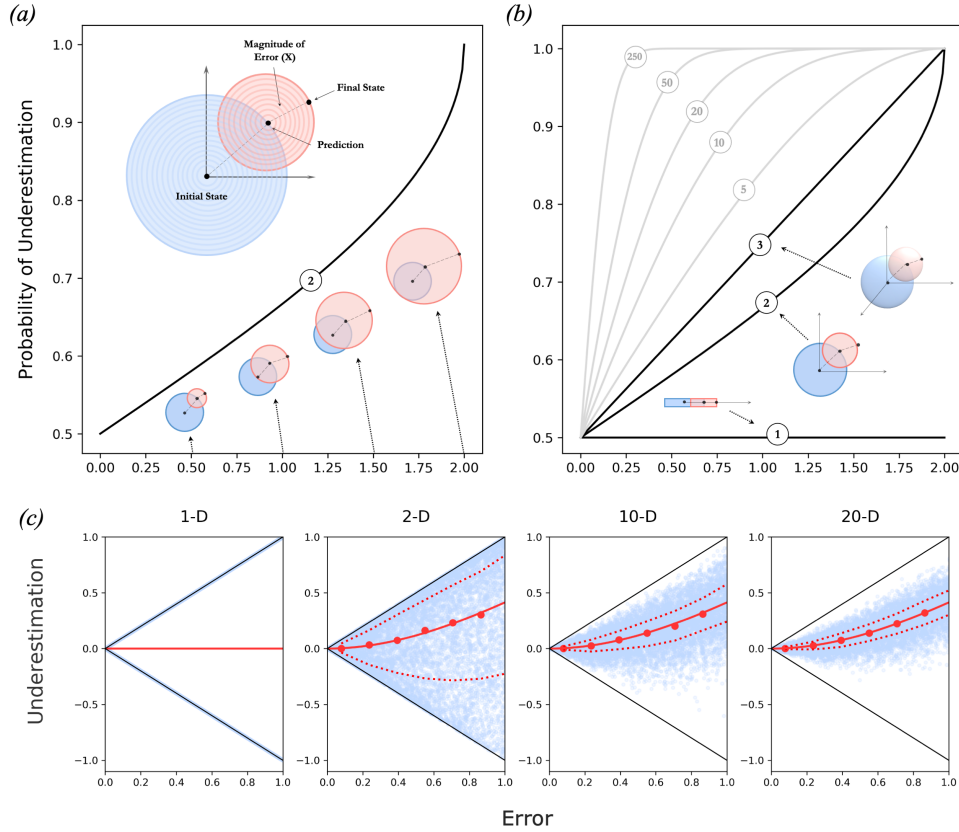


Figure 2: **(a)** Already in two dimensions, the probability of underestimation increases as uncertainty increases. The centre of the blue circle is the initial state (its actual value is irrelevant) and its radius is defined by the predicted magnitude of change. The point at the centre of the red circle corresponds to the predicted state, while its radius represents the magnitude of error made by the prediction. By definition, final states thus fall on the edges of the red circle. If a final state falls inside the blue circle then there has been an overestimation of change (it is closer to the initial state than what was predicted). If a final state falls outside the blue circle (as in the figure) then there has been an underestimation of change (it farther from the initial state than what was predicted). When uncertainty is small, error will be small thus the radius of the red circle is small, and the probability of underestimation is close to 0.5. As uncertainty (thus error) increases, however, there is increasing bias towards underestimation. Eventually when error is twice as large as the prediction only underestimation is possible. **(b)** This relationship between uncertainty and underestimation is strengthened by dimensionality. As dimensions increases there become even more ways to be more different than ways to be more similar. Each curve corresponds to the probability of underestimation as a function of error for different dimensions labeled as circled numbers. For a fixed amount of error the probability of underestimation will increase with dimension. **(c)** The relationship between ~~uncertainty~~ the relative magnitude of error (x) and the relative magnitude of underestimation (y) based on uniform sampling of 1-D, 2-D, 10-D and 20-D intersecting hyper-spheres defined by unbiased but uncertain predictions. The boundaries of this relationship are plotted in black and the mean-median expectation of $y = \sqrt{x^2 + 1} - 1$ $\tilde{y} = \sqrt{x^2 + 1} - 1$ as derived from Eq. (4) is plotted in red (except for 1-D where there is no bias it does not apply). ~~The dashed red lines are the predicted variance of the results based on the number of dimensions.~~ Blue points are simulated results, red points are the actual mean-median values and black points are dashed lines show the actual variances-quantiles for vertical subsets of the simulated data. As dimensionality increases the variance-width of the distribution decreases and results converge-converges towards the expectation its median, which effectively increases the probability of underestimation ~~as can be seen in~~ (b).

136 probability of underestimation is more general and in a sense, simpler. To see that, let us take

137 a step back and analyse the relative magnitude of underestimation, defined as:

$$y = \frac{\|\text{response}\| - \|\text{prediction}\|}{\|\text{prediction}\|} \quad (2)$$

138 Given an angle θ between prediction and error vectors (resp. the vectors that point from initial
139 to predicted state, and from predicted state to realized state) we can rearrange Eq. (2) as:

$$y(x, \theta) = \sqrt{x^2 + 2x \cos(\theta) + 1} - 1 \quad (3)$$

140 the term $\cos \theta$ can take any values between -1 and $+1$. ~~If the uncertainties~~ For the sake of
141 simplicity, in what follows we will suppose that its mean and median are zero. This is the
142 case if the errors associated with individual variables are ~~independent and with zero mean,~~
143 ~~the error vector can point in any direction so that $\cos \theta$ will also have zero mean. Thus, in~~
144 ~~this scenario where prediction of individual components are independent and unbiased, the~~
145 ~~expected~~ drawn from independent symmetric distributions centred on zero (unbiased and
146 unskewed predictions at the component level). In this case the median relationship between
147 error (x) and underestimation (y) is:

$$\tilde{y} = \sqrt{x^2 + 1} - 1 \quad (4)$$

148 which is strictly positive as soon the error x is non zero. This holds true in all dimensions greater
149 than one, which can be seen in Fig. 2c. The ~~mean underestimation \bar{y}~~ median underestimation
150 \tilde{y} does not depend on dimension, but the probability of underestimation, $P(y > 0; x)$, does.
151 Indeed, $P(y > 0; x)$ is driven by the ~~variance of the~~ distribution of the random term $\cos \theta$ in
152 Eq. (3). If this ~~variance is small~~ distribution is narrow, realisations of y will fall close to ~~the~~
153 ~~mean \bar{y}~~ \tilde{y} . Because the latter is positive and increases predictably with x , so will the probability
154 of any realised y to be positive. A known fact from random geometry (~~in particular, about the~~
155 ~~angle between randomly drawn vectors, see Appendix S2) is that the variance of $\cos \theta$ is is~~
156 that, given a random isotropic vector (i.e. a vector whose direction is uniformly distributed
157 on the sphere), its angle θ with any other given vector satisfies

$$\mathbb{E}(\cos \theta) = 0; \text{ and } \text{Var}(\cos \theta) = \frac{1}{S} \quad (5)$$

158 In other words, in high dimensions random vectors are approximately orthogonal, up to a
159 variance inversely proportional to the dimension of state-space:-

$$\underline{\text{Var}(\cos \theta) = \frac{1}{S}}$$

160 ~~In~~. In our context, this corresponds to normal i.i.d. distributions of errors, a particular
 161 case of independent unbiased and unskewed predictions. This explains why the probability
 162 of underestimation increases in Fig. 3b with both dimension S and error x . In what follows
 163 we use ~~this expression~~ the expression for the variance in Eq. (5) as a *definition* of **effective**
 164 ~~dimension.~~ *effective dimension*. In doing so, we ~~have an opportunity to can~~ free ourselves
 165 from the strict Euclidean representation of Fig. 2, ~~which and~~ generalize the theory beyond
 166 ~~i.i.d. normal error distributions.~~ This will be useful when applying our theory to ecological
 167 problems, where components are the biomass of species, are their contribution to ecosystem
 168 change are not equivalent~~-, thus errors not i.i.d.~~

169 3 Relevance to Ecology

170 3.1 Effective Dimensionality

171 We now assume that the axes that define state-space represent the biomass of the species
 172 that form an ecological system. These species may have very different abundances, and thus
 173 will not all contribute equally to a given change. For instance, in response to environmental
 174 perturbations, biomass of species typically change in proportion to their unperturbed values
 175 (Lande, Engen, Saether, et al., 2003; Arnoldi, Bideault, Loreau, & Haegeman, 2018). The
 176 more abundant species (in the sense of higher biomass) will thus likely contribute more to
 177 the ecosystem-level change. Thus, if we use species richness as a measure of dimensionality,
 178 as the above section would suggest, we will surely exaggerate the importance of rare (i.e low
 179 biomass) species. But using Eq. (5) to *define dimensionality*, we can resolve that issue. In
 180 doing so we show that the relevant dimension when applying our ideas to ecological problems
 181 is really a measure of diversity of the community prior to the change, which may not be an
 182 integer, and will typically be smaller than the ~~mere~~ number of individual components.

183 In fact (Appendix S3), if a species contribution to change is statistically proportional to its
 184 biomass B_i the effective dimensionality of a system is the Inverse Participation Ratio (IPR) of
 185 the biomass distribution², which reads:

$$\text{IPR} = \frac{(\sum_{i=1}^S B_i^2)^2}{\sum_{i=1}^S B_i^4} \quad (6)$$

186 This non-integer diversity metric was developed in quantum mechanics to study localisation
 187 of electronic states (Wegner, 1980). The IPR approaches 1 when a single species is much
 188 more abundant than the others, and approaches S when species have similar abundance – see

²our theory allows other choices of statistical relationships between biomass and contribution to change, leading to other diversity metrics, which can be seen as generalization of the Inverse Participation Ratio.

189 Suweis *et al.* (2015) where this metric is used in an ecological context. Note that the IPR is
 190 closely related (but not equivalent) to Hill (1973)'s evenness measure ${}^2D = (\sum_i B_i)^2 / \sum B_i^2$
 191 (see Appendix S3).

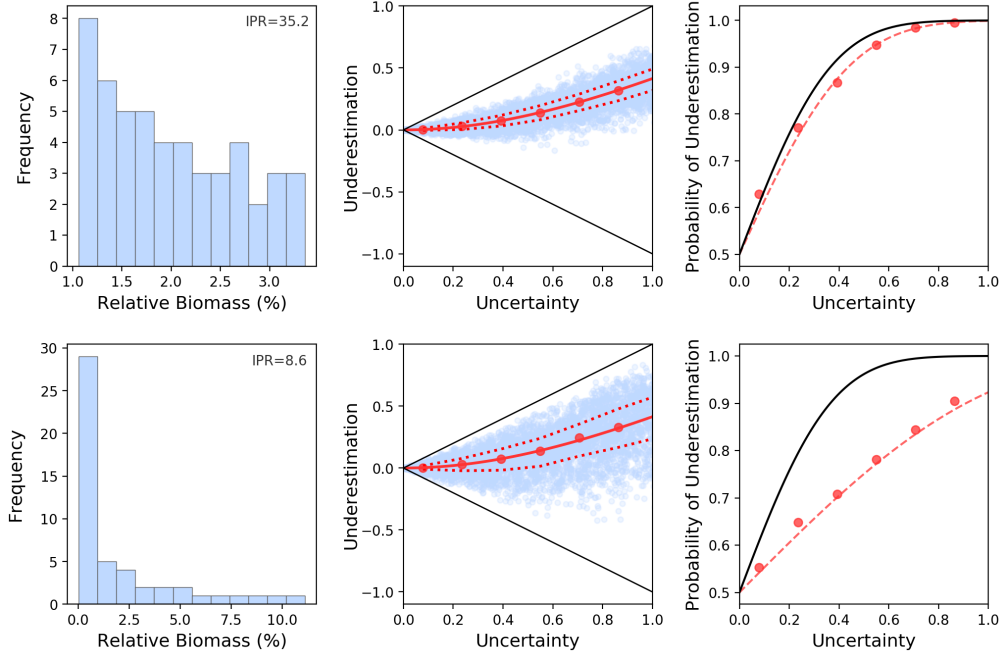


Figure 3: Each row corresponds to simulations of 50 species communities with uneven biomass distributions that have experienced perturbations. The first column shows the biomass distributions of these communities. The two communities have IPR, and therefore effective dimensionality, of 35.2 and 8.6. The second column shows the relationship between error and underestimation of these two communities when unbiased predictions of biomass change are scaled up to change in state-space distance. ~~The variance around the mean expectation was accurately predicted using the IPR instead of species richness.~~ As the biomass distribution becomes more uneven the ~~variance variability~~ around the ~~mean expectation median underestimation~~ increases (~~dashed lines are quantiles~~), which ~~effectively~~ reduces the probability ~~of underestimation that a given change was underestimated~~. This can be seen in the third column where predictions using the dimension of state-space (50, black curves) are outperformed by predictions using the IPR (35.2 and 8.6, red curves). Red points show the actual probabilities of underestimation for vertical subsets of the simulated data and are accurately predicted using the IPR.

192 We can show that it is indeed the IPR that determines the variance (over a sampling of
 193 predictions and associated uncertainties of species biomasses) of the term $\cos \theta$ in Eq. (3) so
 194 that:

$$\text{Var}(\cos \theta) = \frac{1}{\text{IPR}} \quad (7)$$

195 An uneven biomass distribution thus increases the ~~variance of width of the distribution of~~
 196 underestimation y therefore reducing the probability of a given realisation of change to
 197 have been underestimated. ~~As shown~~ ~~If species richness accurately predicted the width of~~
 198 ~~the distribution of underestimation and therefore the probability of underestimation, the two~~
 199 ~~simulated communities~~ in Fig. 3 ~~would behave in the same way. However, the probability~~
 200 ~~of underestimation is lower than expected based on richness, particularly for the community~~

201 with a more uneven biomass distribution. Indeed, replacing richness S by the IPR in Eq. (1)
202 provides an excellent approximation of the behaviour of the probability of underestimation τ
203 (Fig. 3).

204 **3.2 Aggregate Properties and Non-Linearity**

205 When scaling up predictions, there are different ways of measuring system-level change (Box 1).
206 The classic reductionist approach is to quantify change via the Euclidean distance in state-
207 space, thus keeping track of the motion of joint configurations. This is what we have done
208 so far. Ecologically, this could correspond to measuring the absolute biomass change of a
209 community. Here, by construction, our theory is directly relevant.

210 But other, non reductionist, ways of quantifying change at the system-level are possible. In
211 ecology, this could correspond to measuring changes in the diversity, stability or functioning
212 of the ecosystem. Yet, if differences in these properties between two states correlate with the
213 distance in the reductionist state-space, then our theory will remain relevant. As can be seen
214 in Fig. 4 this can be the case for diversity (Shannon's index) and stability (invariability of
215 total biomass (Haegeman et al., 2016)). Our theory thus applies to those ecosystem-level
216 properties. This leads us to the conclusion that their degree of change will be systematically
217 underestimated by predictions built from species-level predictions.

218 On the other hand, changes in ecosystem functioning (total biomass of total biomass (ecosystem
219 functioning) do not correlate well with changes in state-space Euclidean distance. This is
220 due to the fact that total biomass is a linear function of species biomass (i.e. the sum). In
221 fact, quantifying system-level change via a linear function acts as a projection from the state
222 space onto a one-dimensional space defined by the function. Thus, despite the fact that the
223 ecosystem might be constituted of many species (intrinsically high dimensional) the problem
224 of scaling up predictions is essentially one dimensional. As a result, This is why bottom-up
225 predictions of change of total biomass will show no additional bias towards underestimation.

226 More generally, when the linear part of the aggregate property of interest is dominant,
227 dimensional effects are obscured. However, as soon as we consider changes of multiple
228 properties at once, as in multi-functionality approaches in ecology (Box 1), dimensional effects
229 will play out – even if all aggregate properties are essentially linear.

230 **3.3 Multi-Functionality**

231 Scaling up predictions from individual components to an aggregate property can lead to a
232 bias towards underestimation, due to dimensional effects. We explained that this occurs for
233 non-linear aggregate properties, and not linear ones (such as total biomass). Is this to say that

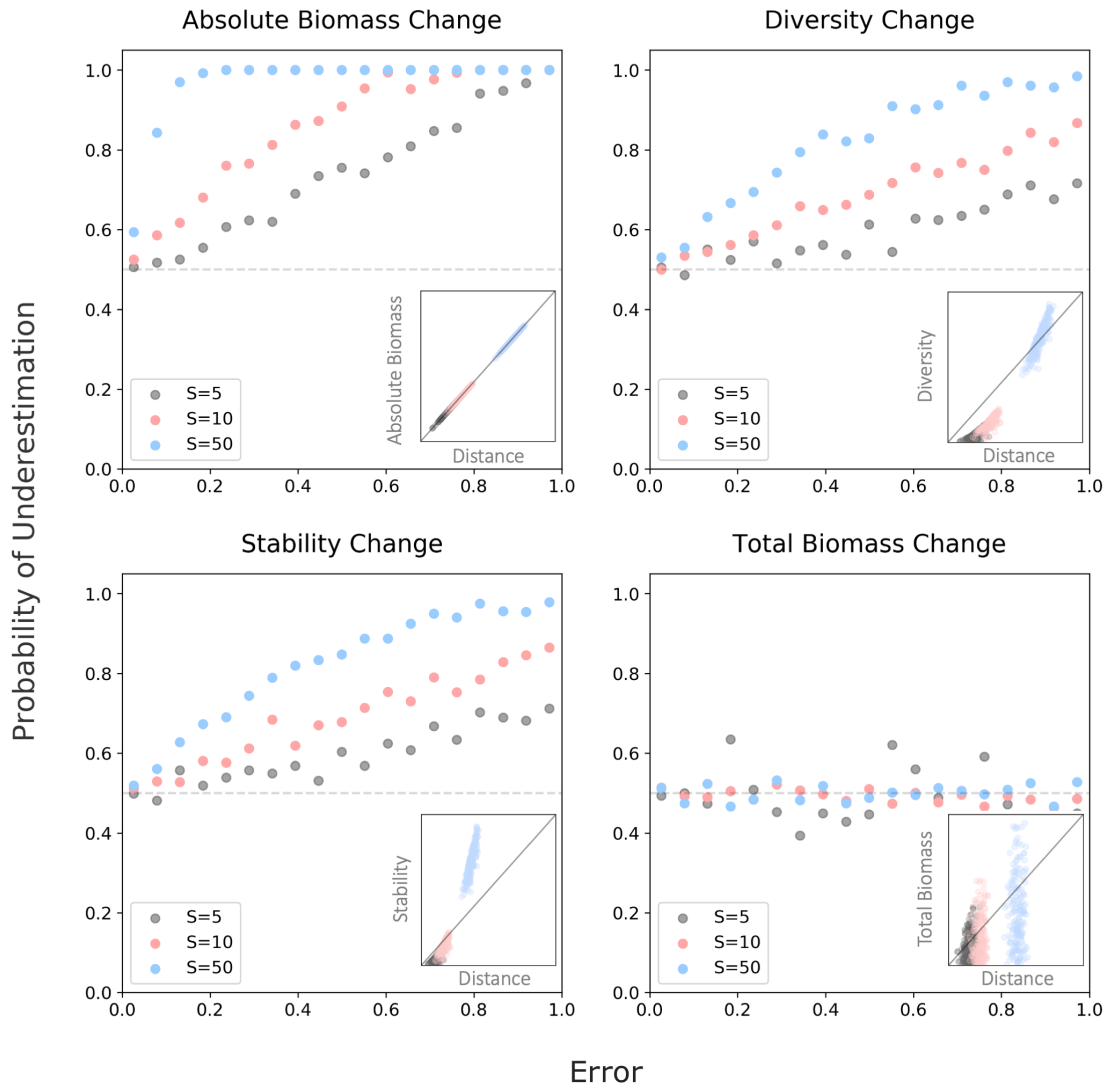


Figure 4: Simulated communities of 5 (grey), 10 (red) and 50 (blue) species experienced some change in their biomass. Unbiased predictions of species' biomass change were scaled up to predictions of change in aggregate properties commonly used in ecological research. The relationship between uncertainty and the probability of underestimation is shown for changes in: (1) absolute biomass, (2) diversity, specifically the Shannon index, (3) stability, specifically invariability and (4) total biomass. Subplots show the relationship between changes in each aggregate property and changes in Euclidean distance. Absolute biomass change is analogous to Euclidean distance. Diversity and stability (non-linear functions) show some correlation with Euclidean distance and are therefore sensitive to dimensional effects. Total biomass (linear function) does not correlate with Euclidean distance so scaled up predictions of change of this aggregate property remain unbiased.

234 our theory is only relevant when predicting the change of non-linear system-level properties?

235 Yes, but only in the restricted realm of one-dimensional approaches to complex systems.

236 There is, in ecology, a growing interest in multi-functionality approaches (Manning et al.,
 237 2018). These approaches are multivariate descriptions of ecosystems, an alternative to the
 238 reductionist perspective to account for the multidimensional nature of ecological systems

239 (Box 1). By considering the change of multiple functions at once, even if these functions are
 240 essentially linear, dimensional effects will resurface.

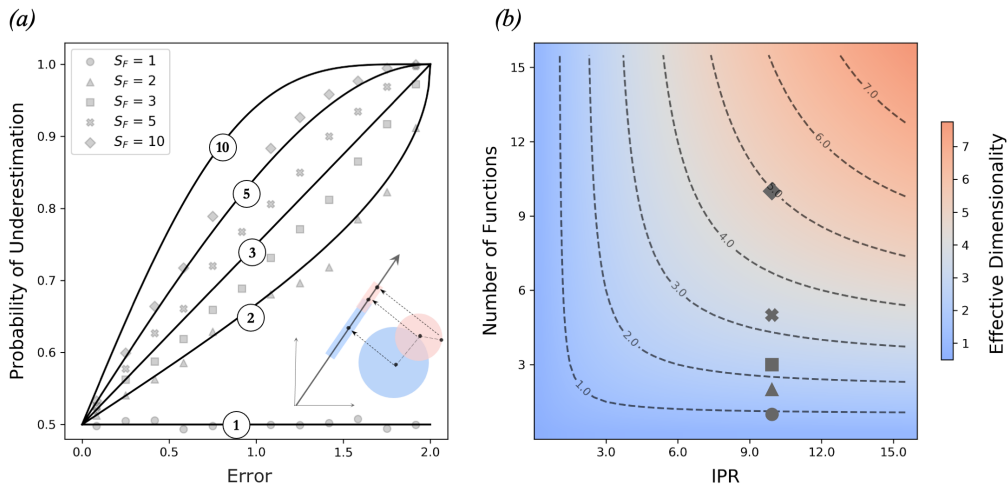


Figure 5: **(a)** The relationship between prediction error caused by uncertainty and the probability of underestimation for five simulations each scaling up predictions to a different number of aggregate properties (S_F). A community of 20 species, with IPR of 9.9, experienced change in biomass over 50,000 simulations. Unbiased predictions at the species level were scaled up to the community level using 1, 2, 3, 5 and 10 randomly drawn aggregate properties. Simulated results fall short of theoretical expectations for the probability of underestimation when the effective dimensionality is presumed to be the number of functions. The blue and red circles being projected onto a blue and red line represents a 2-D system being projected into 1-D functional space. **(b)** There is an interaction between the number of functions and the underlying dimensionality (IPR), which is illustrated by the heat-map. Usually the effective dimensionality is determined by the lower value of S_F and IPR. However, when these values are similar (e.g. diamond: 10 functions and IPR of 9.9) the effective dimensionality (~ 5) is much lower than either value.

241 To be clear, we still assume that we scale up predictions from the species to the ecosystem
 242 level. Only now we scale up predictions from species to several system-level properties at once,
 243 that describe the ecosystem's state from a multi-functional point of view (Box 1). Let us
 244 suppose, for simplicity, that those aggregate properties (or functions) are essentially linear.
 245 We have seen that considering a single linear function, in terms of upscaling of predictions,
 246 essentially reduces the problem to a single dimension. Likewise, considering multiple linear
 247 functions essentially reduces the effective dimensionality to the number of functions. Subtleties
 248 arise when the number of functions (S_f) and the dimensionality of the underlying system (e.g.
 249 IPR) are similar, and/or if the considered functions are colinear (see Appendix S3). For S_f
 250 independent functions measured on a community we find that the effective dimensionality (the
 251 one that determines the probability of underestimation of change) is:

$$S_{\text{eff}} \approx \frac{1}{\frac{1}{\text{IPR}} + \frac{1}{S_f}} \quad (8)$$

252 For example, if the change of an ecosystem with an IPR of 10 is measured using 10 linear
 253 functions at once, the effective dimensionality is ~ 5 (Fig. 5). If functions are colinear the

254 effective dimensionality will be even lower than S_f . This is to be expected, especially when
255 thinking of an extreme case: if we measure the same function multiple times we should see no
256 dimensional effects. In summary, in a multivariate description of complex systems, dimensional
257 effects will inevitably play out, in more or less intricate ways, whenever a prediction is scaled
258 up from individual components to the system-level.

259 4 Discussion

260 Our work demonstrates that a bias towards underestimation of change emerges when predictions
261 of individual components (e.g. species biomass) are scaled up to the system-level (e.g. ecosystem
262 function). Our geometric approach reveals a direct relationship between the probability of
263 underestimation, the magnitude of error caused by uncertainty and a system's effective
264 dimensionality. We noted that the effective dimensionality is not necessarily the number of
265 individual components that form a system, but rather a measure of diversity *sensu* Hill (1973).
266 In essence, these results come from the fact that *in high dimensions there are more ways to be*
267 *more different, than ways to be more similar* ~~—(Fig. 6)~~. Our goal was to make this remark
268 quantitative and generally relevant to ecological problems.

269 We explained why it is non-linear aggregate properties (e.g. absolute biomass change, stability
270 or diversity) that are sensitive to dimensional effects ~~—(Fig. 6)~~. For linear properties (e.g. total
271 biomass), scaling up does not generate bias. Yet, even in this case, dimensional effects will
272 play out if several functions are considered at once to describe the ~~state-of-a-system-ecosystem,~~
273 as in multi-functional approaches in ecology.

274 Natural systems are intrinsically complex and the way that we describe them is necessarily
275 multivariate (Loreau, 2010). It is generally accepted, in ecology, that there is a need for
276 mechanistic predictive models, built from individual components and scaled up to the ecosystem-
277 level (Poff, 1997; Mouquet et al., 2015; Harfoot et al., 2014; Woodward et al., 2010). We
278 have shown that dimensional effects will play out in this scaling-up, generating additional bias
279 towards underestimation of any predicted system-level change. This is not to say that scaling
280 up predictions is a faulty approach, rather that one must keep track of dimensional effects
281 when doing so. ~~Our work provides generic expectations needed to appropriately interpret~~
282 ~~predictions of mechanistic models.~~

283 Our theory provides a generic expectation for the consequences of uncertainty when predictions
284 are scaled up from individual components to the system as a whole. As a result, it provides
285 a baseline, of what to expect if only dimensional effects are at play, against which we can
286 test biological (or other) effects. To inform empirical work, it is important to recognise
287 that there are two ways that a result can deviate from our generic expectation. Focusing

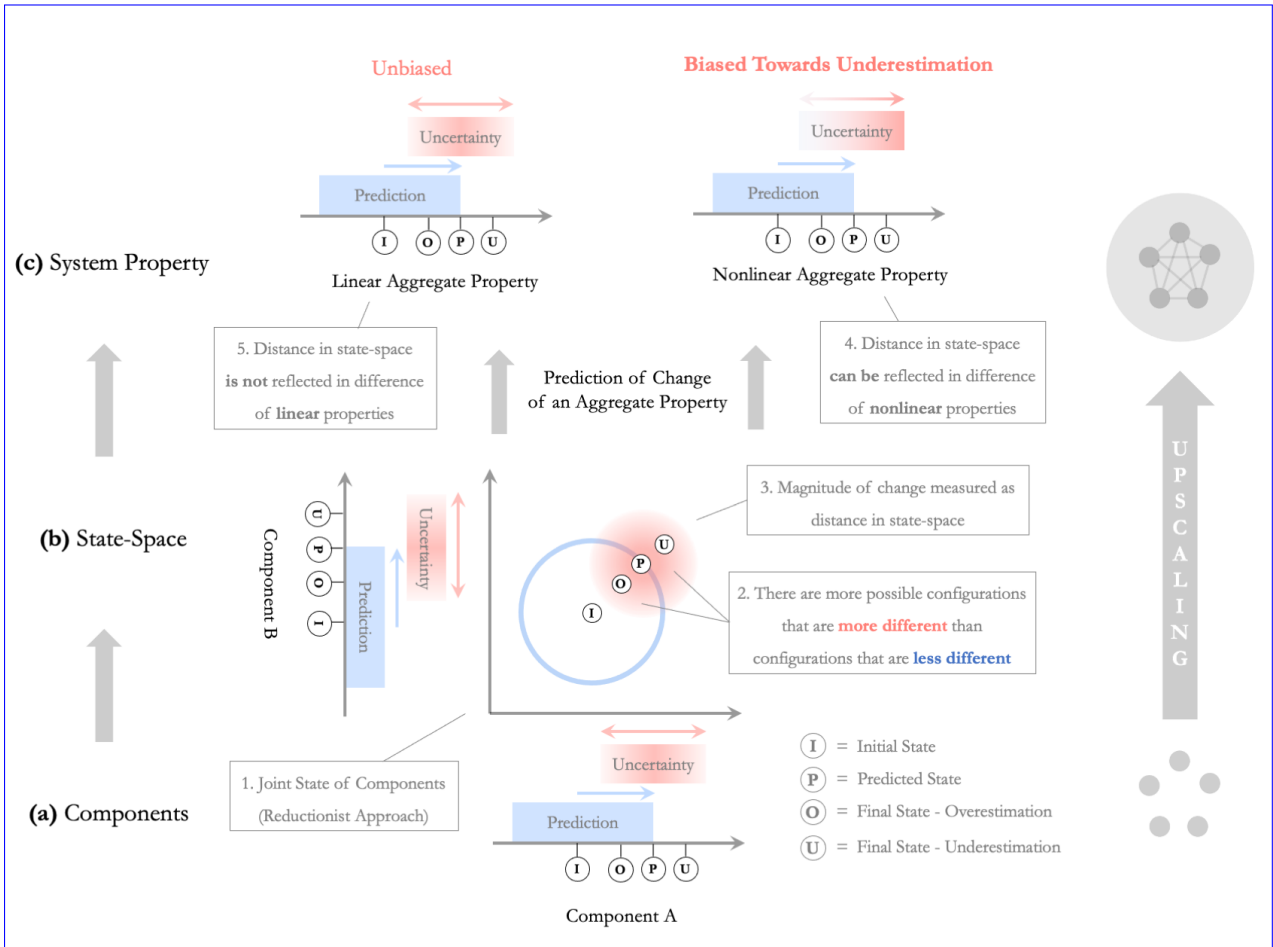


Figure 6: An overview our of main findings. (a) Two components, A and B are (b) considered at once to define a joint state (I). Suppose this state changes and falls near a predicted state (P). Then there are more ways for this state to be more different from (I), than ways to be more similar; more of the red disk is outside the blue circle than inside. Consequently, when predictions of change (blue) for individual components are scaled up to predictions of change of their joint state, unbiased uncertainties (red) become biased towards underestimation. In section *Geometric Approach* we quantified these surprising dimensional effects and investigate beyond the basic two-dimensional case shown here. (c) Magnitude of system-level change can be measured as distance in state space or by some other aggregate property. If an aggregate property is sensitive to changes in distance of the underlying state-space, dimensional effects, and therefore a bias towards underestimation, will be conserved. As we explained in section *Aggregate Properties and Non-Linearity*, it is the non-linear part of an aggregate property that controls its sensitivity to changes in state-space distance and thus the tendency of its degree of change to be underestimated by upscaled predictions.

288 on the relationship between uncertainty and underestimation of change shown in Figs. 2-3,
 289 the mean-median can be shifted due to a systematic bias caused by interactions between
 290 component uncertainties, which are assumed independent and in our framework. Furthermore,
 291 the variance-around-this-mean-distribution around this median can be more than or less than
 292 expected, which indicates either wrong estimation of effective dimensionality, or a systematic
 293 effect caused by something other than geometry —(e.g. skewed distributions of errors or
 294 interactions). Having a clear baseline against which to identify non-geometric effects can
 295 improve our understanding of complex systems.

296 We only considered two levels of organisation: the level where predictions are made and the
297 level where predictions are scaled up to. However, intermediate levels could, in principle,
298 be considered. For instance, given the increasing resolution of ecological data, predictions
299 of change may originally be based at the level of individual organisms and could first be
300 scaled up to species-level predictions and subsequently scaled up to ecosystem-level predictions.
301 Here, if non-linear aggregate properties are used, dimensional effects will bias species-level
302 predictions towards underestimation and will further increase this bias for ecosystem-level
303 predictions. With an ever-increasing resolution of data, scaling predictions across multiple
304 levels of organisation, and potentially introducing dimensional effects at multiple levels, may
305 become more common in the study of complex systems.

306 Our work is theoretical and, in essence abstract. Yet it may be relevant for highly practical
307 domains of ecology. To make this point, we will now discuss some implications of our theory
308 to multiple-stressor ecological research, an essentially empirical field that explicitly deals with
309 considerable uncertainty of predictions and holds great interest in its consequences.

310 4.1 Multiple-Stressor Research

311 In the light of our theory, we ~~now propose to~~ revisit a seemingly unrelated ~~question~~ problem of
312 wide ecological interest: what is the combined effect of multiple stressors on a given ecosystem?
313 By translating our theory into the language of multiple-stressor research we aim to highlight
314 some implications and to inspire further generalization.

315 The combined effect of stressors on an ecological system ~~of interest~~ is generally predicted based
316 on the sum of their isolated effects ~~using~~, i.e. an “additive null model” (Folt, Chen, Moore, &
317 Burnaford, 1999; Schäfer & Piggott, 2018). Uncertainty ~~of~~ around this additive prediction,
318 which is ubiquitous in empirical studies (Crain, Kroeker, & Halpern, 2008; Jackson et al., 2016;
319 Holmstrup et al., 2010), causes prediction errors called “non-additivity”. Uncertain predictions
320 will either overestimate or underestimate the combined effect of stressors, respectively creating
321 “antagonism” and “synergism” (Folt et al., 1999; Piggott et al., 2015). This translation ~~will of~~
322 stressor interactions in terms of prediction uncertainty and under- or over-estimation lead us
323 to the conclusion that scaling up uncertain multiple-stressor predictions ~~will generate~~ generates
324 bias towards synergism.

325 ~~In this context~~ Here, scaling up predictions refers to multiple-stressor predictions (e.g. an
326 additive model) at one level (e.g., individuals, populations) being used to build multiple-
327 stressor predictions at higher levels of biological organisation (e.g. communities, ecosystems),
328 an approach for which there is growing interest (Orr et al., 2020; Thompson, MacLennan, &
329 Vinebrooke, 2018; Kroeker, Kordas, & Harley, 2017; Côté et al., 2016). To be clear, scaling up

330 predictions is not equivalent to simply scaling up investigations; our theory does not predict
331 greater synergism at higher levels of organisation. ~~If, however, multiple-stressor predictions~~
332 ~~of~~ In fact, we are not making predictions about how stressors will behave at higher levels of
333 organization. What we claim instead is that, if we have a model for the combined effect of
334 stressors at one level of organization and use that model to deduce their combined effect at
335 higher levels, the process of scaling up the model will introduce a ~~system are constructed from~~
336 ~~the bottom up (i.e. reductionist approach)~~ ~~a bias towards synergism emerges in a predicable~~
337 ~~way~~ an observed synergy between stressors, even if no systematic synergy was observed at the
338 lower level.

339 Our theory has consequences for the interpretation of stressor interactions and is therefore
340 relevant to the debate surrounding multiple-stressor null models (Griffen, Belgrad, Cannizzo,
341 Knotts, & Hancock, 2016; Liess, Foit, Knillmann, Schäfer, & Liess, 2016; De Laender, 2018;
342 Schäfer & Piggott, 2018). Our findings are especially relevant to the *Compositional Null Model*,
343 which employs a reductionist approach to the construction of multiple-stressor predictions
344 (Thompson et al., 2018). In such an approach, the baseline against which biological effects are
345 tested must be shifted. Dimensional effects, quantified by the effective dimensionality of the
346 underlying system and the non-linearity of aggregate properties, need to be accounted for to
347 decipher a biological synergism from merely a statistical synergism.

348 4.2 Conclusions

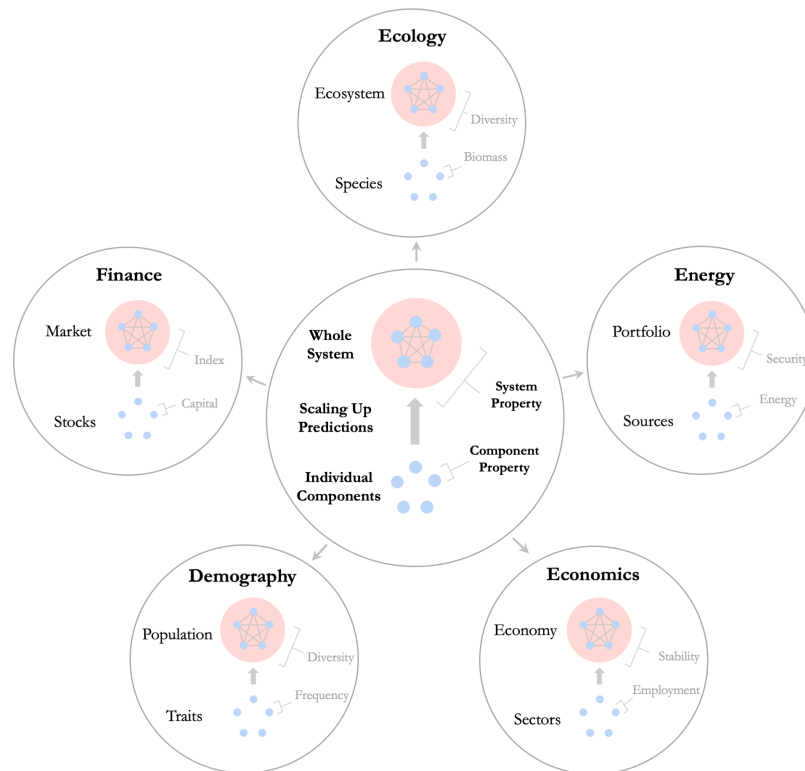
349 In this paper we have addressed a subproblem of the reductionist program (Levins & Lewontin,
350 1985; Wan, 2013; Loreau, 2010). We investigated the consequences of uncertainty when
351 unbiased predictions of individual components are scaled up to predictions of system-level
352 change. Due to a geometric observation that *in high dimensions there are more ways to be more*
353 *different, than ways to be more similar*, scaling up uncertain predictions can underestimate
354 system-level change. These dimensional effects manifest when non-linear, but not linear,
355 aggregate properties are used to measured change at the system level, and when multiple
356 functions are considered at once. Although we have primarily focused on ecology, and in
357 particular on the response of ecosystems to perturbations; our general findings could inform any
358 field of science where predictions about whole systems are constructed from joint predictions
359 on their individual components, such as economics, finance, energy supply, and demography
360 (Box 2).

361 Acknowledgements

362 We thank Matthieu Barbier, Nuria Galiana and Yuval Zelnik for discussions and review of
363 previous versions of this work. JFA and ALJ were supported by an Irish Research Council

³⁶⁴ Laureate Award IRCLA/2017/186. JO was supported by an Irish Research Council Laureate
³⁶⁵ Award IRCLA/2017/112 and TCD Provost's PhD Award held by JP.

Box 2: Generalisation Beyond Ecology



Scaling up prediction to higher levels of organisation is not unique to ecology. Our basic Our findings could be relevant to other fields of science – Whenever where: (i) there is interest in predicting change of complex systems based on knowledge about their individual components, and (ii) systems are described using multivariate coordinates and/or using non-linear properties of individual components.

- In **economics**, a region's economy can be viewed as a complex system comprised of individual sectors (e.g. agriculture, tourism, technology). Predictions of how employment numbers will change in individual sectors due to some perturbation could be scaled up to predictions of change of economy-level properties of interest such as stability, measured as, for example, the evenness of employment across sectors (Halpern et al., 2012; Malizia & Ke, 1993; Dissart, 2003).
- In the study of **energy supply**, different fuel or energy sources of a country (e.g. solar, wind, oil) can be considered together in a country's energy portfolio. Predictions of change of energy generation in each individual source could be scaled up to predictions of change of portfolio-level properties. Energy security is a system-level property of great interest that is quantified using diversity metrics (Stirling, 1994; Chalvatzis & Ioannidis, 2017) or variance-based approaches (Roques, Newbery, & Nuttall, 2008) based on *Mean-Variance Portfolio Theory*, which was originally developed to study risk or volatility of investment portfolios (Markowitz & Todd, 2000).
- In **demography**, populations can be thought of as systems comprised of multiple different groups that are defined by traits (e.g. gender, age, ethnicity). Again, diversity is a system-level property of great interest in the study of populations that is quantified using non-linear aggregate functions (Reardon & Firebaugh, 2002; White, 1986). Changes in diversity of human populations is pertinent to many social sciences including **sociology, economics and politics**.
- In **finance**, markets are complex systems whose individual components are stocks. Predictions of how the capital of individual stocks will change could be scaled up to predictions of how stock market indices will change. Certain stock market indices, for example diversity-weighted indices, are non-linear aggregate properties that will be sensitive to dimensional effects (Fernholz, Garvy, & Hannon, 1998; Chow, Hsu, Kalesnik, & Little, 2011). At a different financial scale, our theory may also be relevant to the study of investment portfolios. Here, analogous to energy security, portfolios are systems comprised of individual assets and the volatility or risk tolerance of a portfolio (measured using non-linear aggregate properties) is of great interest to investors (Markowitz & Todd, 2000; Bera & Park, 2008).

References

- Arnoldi, J.-F., Bideault, A., Loreau, M., & Haegeman, B. (2018). How ecosystems recover from pulse perturbations: A theory of short-to long-term responses. *Journal of theoretical biology*, *436*, 79–92.
- Bera, A. K., & Park, S. Y. (2008). Optimal portfolio diversification using the maximum entropy principle. *Econometric Reviews*, *27*(4-6), 484–512.
- Chalvatzis, K. J., & Ioannidis, A. (2017). Energy supply security in the eu: Benchmarking diversity and dependence of primary energy. *Applied Energy*, *207*, 465–476.
- Chow, T.-m., Hsu, J., Kalesnik, V., & Little, B. (2011). A survey of alternative equity index strategies. *Financial Analysts Journal*, *67*(5), 37–57.
- Côté, I. M., Darling, E. S., & Brown, C. J. (2016). Interactions among ecosystem stressors and their importance in conservation. *Proceedings of the Royal Society B: Biological Sciences*, *283*(1824), 20152592.
- Crain, C. M., Kroeker, K., & Halpern, B. S. (2008). Interactive and cumulative effects of multiple human stressors in marine systems. *Ecology Letters*, *11*(12), 1304–1315.
- De Laender, F. (2018). Community-and ecosystem-level effects of multiple environmental change drivers: Beyond null model testing. *Global Change Biology*, *24*(11), 5021–5030.
- Dissart, J. C. (2003). Regional economic diversity and regional economic stability: research results and agenda. *International Regional Science Review*, *26*(4), 423–446.
- Dovers, S. R., & Handmer, J. W. (1992). Uncertainty, sustainability and change. *Global Environmental Change*, *2*(4), 262–276.
- Fernholz, R., Garvy, R., & Hannon, J. (1998). Diversity-weighted indexing. *Journal of Portfolio Management*, *24*(2), 74.
- Folt, C., Chen, C., Moore, M., & Burnaford, J. (1999). Synergism and antagonism among multiple stressors. *Limnology and Oceanography*, *44*(3part2), 864–877.
- Griffen, B. D., Belgrad, B. A., Cannizzo, Z. J., Knotts, E. R., & Hancock, E. R. (2016). Rethinking our approach to multiple stressor studies in marine environments. *Marine Ecology Progress Series*, *543*, 273–281.
- Haegeman, B., Arnoldi, J.-F., Wang, S., de Mazancourt, C., Montoya, J. M., & Loreau, M. (2016). Resilience, invariability, and ecological stability across levels of organization. *bioRxiv*, 085852.
- Halpern, B. S., Longo, C., Hardy, D., McLeod, K. L., Samhouri, J. F., Katona, S. K., . . . others (2012). An index to assess the health and benefits of the global ocean. *Nature*, *488*(7413), 615–620.
- Harfoot, M. B., Newbold, T., Tittensor, D. P., Emmott, S., Hutton, J., Lyutsarev, V., . . . Purves, D. W. (2014). Emergent global patterns of ecosystem structure and function

402 from a mechanistic general ecosystem model. *PLoS Biology*, 12(4).

403 Hill, M. O. (1973). Diversity and evenness: A unifying notation and its consequences. *Ecology*,
404 54(2), 427-432. doi: 10.2307/1934352

405 Holmstrup, M., Bindesbøl, A.-M., Oostingh, G. J., Duschl, A., Scheil, V., Köhler, H.-R., ...
406 others (2010). Interactions between effects of environmental chemicals and natural
407 stressors: a review. *Science of the Total Environment*, 408(18), 3746-3762.

408 Jackson, M. C., Loewen, C. J., Vinebrooke, R. D., & Chimimba, C. T. (2016). Net effects
409 of multiple stressors in freshwater ecosystems: a meta-analysis. *Global Change Biology*,
410 22(1), 180-189.

411 Kroeker, K. J., Kordas, R. L., & Harley, C. D. (2017). Embracing interactions in ocean
412 acidification research: confronting multiple stressor scenarios and context dependence.
413 *Biology Letters*, 13(3), 20160802.

414 Lande, R., Engen, S., Saether, B.-E., et al. (2003). *Stochastic population dynamics in ecology
415 and conservation*. Oxford University Press on Demand.

416 Levins, R., & Lewontin, R. C. (1985). *The dialectical biologist*. Harvard University Press.

417 Liess, M., Foit, K., Knillmann, S., Schäfer, R. B., & Liess, H.-D. (2016). Predicting the
418 synergy of multiple stress effects. *Scientific Reports*, 6, 32965.

419 Loreau, M. (2010). *From populations to ecosystems: Theoretical foundations for a new
420 ecological synthesis (mpb-46)* (Vol. 46). Princeton University Press.

421 Malizia, E. E., & Ke, S. (1993). The influence of economic diversity on unemployment and
422 stability. *Journal of Regional Science*, 33(2), 221-235.

423 Manning, P., van der Plas, F., Soliveres, S., Allan, E., Maestre, F. T., Mace, G., ... Fischer,
424 M. (2018). Redefining ecosystem multifunctionality. *Nature Ecology & Evolution*, 2(3),
425 427-436.

426 Markowitz, H. M., & Todd, G. P. (2000). *Mean-variance analysis in portfolio choice and
427 capital markets* (Vol. 66). John Wiley & Sons.

428 Mouquet, N., Lagadeuc, Y., Devictor, V., Doyen, L., Duputié, A., Eveillard, D., ... others
429 (2015). Predictive ecology in a changing world. *Journal of Applied Ecology*, 52(5),
430 1293-1310.

431 Orr, J. A., Vinebrooke, R. D., Jackson, M. C., Kroeker, K. J., Kordas, R. L., Mantyka-Pringle,
432 C., ... others (2020). Towards a unified study of multiple stressors: divisions and
433 common goals across research disciplines. *Proceedings of the Royal Society B*, 287(1926),
434 20200421.

435 Petchey, O. L., Pontarp, M., Massie, T. M., Kéfi, S., Ozgul, A., Weilenmann, M., ... others
436 (2015). The ecological forecast horizon, and examples of its uses and determinants.
437 *Ecology Letters*, 18(7), 597-611.

438 Piggott, J. J., Townsend, C. R., & Matthaei, C. D. (2015). Reconceptualizing synergism and

- 439 antagonism among multiple stressors. *Ecology and Evolution*, 5(7), 1538–1547.
- 440 Poff, N. L. (1997). Landscape filters and species traits: towards mechanistic understanding
441 and prediction in stream ecology. *Journal of the North American Benthological Society*,
442 16(2), 391–409.
- 443 Reardon, S. F., & Firebaugh, G. (2002). Measures of multigroup segregation. *Sociological*
444 *Methodology*, 32(1), 33–67.
- 445 Roques, F. A., Newbery, D. M., & Nuttall, W. J. (2008). Fuel mix diversification incentives
446 in liberalized electricity markets: A mean–variance portfolio theory approach. *Energy*
447 *Economics*, 30(4), 1831–1849.
- 448 Schäfer, R. B., & Piggott, J. J. (2018). Advancing understanding and prediction in multiple
449 stressor research through a mechanistic basis for null models. *Global Change Biology*,
450 24(5), 1817–1826.
- 451 Stirling, A. (1994). Diversity and ignorance in electricity supply investment: Addressing the
452 solution rather than the problem. *Energy Policy*, 22(3), 195–216.
- 453 Suweis, S., Grilli, J., Banavar, J. R., Allesina, S., & Maritan, A. (2015). Effect of localization
454 on the stability of mutualistic ecological networks. *Nature Communications*, 6, 10179.
- 455 Thompson, P. L., MacLennan, M. M., & Vinebrooke, R. D. (2018). An improved null model
456 for assessing the net effects of multiple stressors on communities. *Global Change Biology*,
457 24(1), 517–525.
- 458 Wan, P. Y.-z. (2013). Dialectics, complexity, and the systemic approach: Toward a critical
459 reconciliation. *Philosophy of the Social Sciences*, 43(4), 411–452.
- 460 Wegner, F. (1980). Inverse participation ratio in $2+ \varepsilon$ dimensions. *Zeitschrift für Physik B*
461 *Condensed Matter*, 36(3), 209–214.
- 462 White, M. J. (1986). Segregation and diversity measures in population distribution. *Population*
463 *Index*, 198–221.
- 464 Woodward, G., Perkins, D. M., & Brown, L. E. (2010). Climate change and freshwater
465 ecosystems: impacts across multiple levels of organization. *Philosophical Transactions*
466 *of the Royal Society B: Biological Sciences*, 365(1549), 2093–2106.
- 467 Wu, J., Jones, B., Li, H., & Loucks, O. L. (2006). *Scaling and uncertainty analysis in ecology*.
468 Springer.

Supporting Information

471 James Orr, Jeremy Piggott, Andrew Jackson, and Jean-François Arnoldi

472 S1 Geometrical model

473 Consider a complex system whose states are given by points in \mathbb{R}^S (thus determined by S
 474 individual variables, e.g species biomass). Let $v \in \mathbb{R}^S$ be an expectation for a change of state.
 475 Let w be the actual change that is observed, and define the error vector u such that $w = v + u$.
 476 From u and v we define a scalar measure x of relative error as

$$x = \frac{\|u\|_2}{\|v\|_2}$$

477 We formalize the question of whether there has been more change observed than predicted, by
 478 defining

$$y = \frac{\|w\|_2 - \|v\|_2}{\|v\|_2}$$

479 In both of the above expressions $\|\cdot\|_p$ denotes the L_p norm of vectors. $p = 2$ corresponds to
 480 Euclidean distance, we ~~still~~ still see below that other values of p can occur in our formalism.
 481 Also, our results hold for other choices of norm in defining x and y . The Euclidian norm is
 482 however, the most convenient for a geometrical approach. A reorganization of y gives

$$y = y(x, \theta) = \sqrt{1 + x^2 + 2x \cos \theta} - 1$$

483 where θ is the angle between error u and prediction v , that is

$$\cos \theta = \frac{\langle u|v \rangle}{\|u\|_2 \|v\|_2}$$

484 S2 Random ensemble

485 We now assume that u and v are random variables (but the prediction v could also be given).
 486 We assume however that the components of u_i have zero mean ~~the and median the~~ prediction
 487 of individual variables is unbiased and unskewed. Then $\mathbb{E}_u \langle u|v \rangle = 0$, thus $\mathbb{E} \cos \theta = 0$. This

488 implies that

$$\underline{\mathbb{E}M}_u y \approx \sqrt{1+x^2} - 1$$

489 At fixed error x , the ~~variance of underestimation y is thus approximately proportional to~~
 490 ~~distribution around this median is driven by~~ variance of $\cos \theta$, over random draws of vectors
 491 u and v . We first define the covariance matrices $C^u = (C_{ij}^u) = \mathbb{E}_u (u_i u_j)$, and $C^v = (C_{ij}^v) =$
 492 $\mathbb{E}_v (v_i v_j)$. We then have that

$$\begin{aligned} \mathbb{E}_{u,v} \langle u|v \rangle^2 &= \mathbb{E}_{u,v} \langle v|u \rangle \langle u|v \rangle \\ &= \mathbb{E}_v \langle v|C^u v \rangle \\ &= \text{Tr} C^u C^v \end{aligned}$$

493 and similarly

$$\mathbb{E}_{u,v} \|u\|^2 \|v\|^2 = \text{Tr} C^u \text{Tr} C^v$$

494 Thus

$$\mathbb{E} \cos^2 \theta \simeq \frac{\text{Tr} C^u C^v}{\text{Tr} C^u \text{Tr} C^v} \quad (\text{S1})$$

495 Example

496 Suppose that $C_u = \sigma^2 \mathbb{I}$ where \mathbb{I} is the identity matrix. This implies that uncertainties of the
 497 individual variables are independent random variables with ~~similar variance~~ variance σ^2 . We
 498 then have

$$\mathbb{E}_u \langle u|v \rangle^2 = \sigma^2 \|v\|^2$$

499 while

$$\mathbb{E}_u \|u\|^2 = S \sigma^2$$

500 so that

$$\mathbb{E}_u \cos^2 \theta \simeq \frac{1}{S}$$

501 S2.1 Probability of underestimation

502 Given an imprecision level x , the theory has underestimated the actual response if $y(x, \theta) \geq 0$
 503 and thus if the angle θ between the theoretical prediction v and the vector of unaccounted
 504 change u satisfies

$$\cos \theta \geq -\frac{x}{2}$$

505 If $\cos \theta$ is approximately normally distributed with zero mean and variance $\sigma^2 = \frac{1}{S}$, than

$$\mathbb{P}(y \geq 0 : x) \simeq \frac{1}{\sqrt{2\pi\sigma^2}} \int_{-\frac{x}{2}}^{\infty} \exp\left(-\frac{s^2}{2\sigma^2}\right) ds$$

506 hence, by the properties of the cumulative distribution function of standard normal distributions,
 507 one gets

$$\mathbb{P}(y \geq 0 : x) \simeq \frac{1}{2} \left[1 + \operatorname{erf} \left(\frac{x}{2} \sqrt{\frac{S}{2}} \right) \right]$$

508 where erf is the error function. This expression should be compared to the exact solution
 509 in the case of a uniform sampling over the direction of u (which is the case if $u_i \sim \mathcal{N}(0, 1)$
 510 –uncertainties of individual variables are independent and normally distributed). In this special
 511 case the problem of deriving the probability of synergism-underestimation becomes purely
 512 geometrical: it is the surface of a ball of radius x and centered on the unit sphere, that is
 513 contained in the unit ball. One then gets

$$\mathbb{P}(y \geq 0 : x) = 1 - \frac{1}{2} I_{1-\frac{x^2}{2}} \left(\frac{S-1}{2}; \frac{1}{2} \right)$$

514 Where $I_s(a, b)$ is the regularized β -function (the cumulative distribution of the β -distribution).
 515 In fact those two expression converge at high diversity S . In any case, we see here that the
 516 probability of underestimation will grow with S .

517 **S3 Effective diversity**

518 S may not always be the relevant measure of diversity. Indeed if $u_i = N_i^{\frac{p}{2}} u'_i$ where N_i is the
 519 abundance (or biomass) of species i and $C^{u'} \propto \mathbb{I}$ then $C^u \propto D^p$ where D is a diagonal matrix
 520 with $D_{ii} = N_i$. If v_i obeys a similar rule, so that $C^v \propto D^q$ then

$$\operatorname{Tr} C^u C^v \propto \|N\|_{\frac{p+q}{p+q}}^{p+q}$$

521 while

$$\operatorname{Tr} C^u \operatorname{Tr} C^v \propto \|N\|_p^p \|N\|_q^q$$

522 so that

$$\mathbb{E} \cos^2 \theta \simeq \frac{\|N\|_{\frac{p+q}{p+q}}^{p+q}}{\|N\|_q^q \|N\|_p^p} =: \frac{1}{\operatorname{IPR}_{q,p}(N)}$$

523 In particular, for $q = p = 2$ we get that

$$\mathbb{E} \cos^2 \theta \simeq \frac{1}{\operatorname{IPR}(N)}$$

524 where $\operatorname{IPR}(N)$ is the Inverse Participation Ratio, a measure of diversity of the abundance
 525 distribution N . The more general expression above can also be seen as a measure of effective

526 diversity. It can be compared to Hill's diversity metrics with index $Q = p + q$

$${}^Q D = \left(\sum p_i^Q \right)^{\frac{1}{1-Q}} = \left(\frac{\|N\|_1}{\|N\|_Q} \right)^{\frac{Q}{Q-1}} = \left(\frac{\|N\|_1^p \|N\|_1^q}{\|N\|_{p+q}^{p+q}} \right)^{\frac{1}{p+q-1}}$$

527 where p_i is the relative abundance of species i . We indeed see that ${}^Q D$ coincides with $\text{IPR}_{q,p}$
 528 when $q = p = 1$, and stays closely related in general. In fact, using the inequality

$$\|N\|_p \leq \|N\|_1 \leq S^{1-\frac{1}{p}} \|N\|_p; \quad p \geq 1$$

529 one gets, for $p, q \geq 1$

$$S^{2-Q} \times {}^Q D^{Q-1} \leq \text{IPR}_{q,p} \leq {}^Q D^{Q-1}$$

530 S3.1 Probability of underestimation

531 If $\cos \theta$ is approximately normally distributed with zero mean and variance $\sigma^2 = \frac{1}{S_{\text{eff}}}$ (where
 532 $S_{\text{eff}} \leq S$ would be an effective dimensionality as defined in the previous sections), than

$$\mathbb{P}(y \geq 0 : x) \simeq \frac{1}{2} \left[1 + \text{erf} \left(\frac{x}{2} \sqrt{\frac{S_{\text{eff}}}{2}} \right) \right]$$

533 This expression should be compared to the exact solution derived above in the case of a
 534 uniform sampling over the direction of u (the case if $u_i \sim \mathcal{N}(0, 1)$), which suggest the Ansatz

$$\mathbb{P}(y \geq 0 : x) = 1 - \frac{1}{2} I_{1-\frac{x^2}{2}} \left(\frac{S_{\text{eff}} - 1}{2}; \frac{1}{2} \right)$$

535 when the effective dimensionality is not necessarily S or even an integer (the two expressions
 536 uniformly converge towards one another as S_{eff} grows).

537 S3.2 Projection on linear functions

538 Suppose now that we measure S_F linear functions ~~F_α~~ of species biomass ~~of the form~~

$$F_\alpha(B) = \sum_{i=1}^S F_{\alpha,i} B_i \quad \alpha = 1, \dots, S_F$$

539 We must now project the covariance matrices onto the space spanned by the gradient ~~if~~ $(F_{\alpha,i})$
 540 of the functions. If $P_\alpha = (F_{\alpha,i}F_{\alpha,j})$ the projector on the function F_α , we can do this as

$$\mathbb{E}_{u,v} \cos^2 \theta_F \simeq \frac{\sum_{\alpha,\beta} \text{Tr} P_\alpha C^u P_\beta C^v}{\sum_{\alpha,\beta} \text{Tr} P_\alpha C^u \text{Tr} P_\beta C^v}$$

541 When taking an ensemble average of functions, with $\mathbb{E}P_\alpha = \mathcal{P} = (\mathbb{E}F_i F_j)$, we must take care
 542 in differentiating terms in sums for which $\alpha \neq \beta$ and terms where $\alpha = \beta$. In the former case
 543 the projectors P_α and P_β are independent random variables and we can replace them by their
 544 mean \mathcal{P} . In the latter case, we must first define \hat{P}_α as the linear operator that maps a matrix
 545 M to $P_\alpha M P_\alpha$; its ensemble mean $\hat{\mathcal{P}}$ encodes the 4th moments of F_α . We then get

$$\mathbb{E} \cos^2 \theta_F \simeq \frac{(S_F - 1) \text{Tr} \mathcal{P} C^u \mathcal{P} C^v + \text{Tr} \hat{\mathcal{P}}(C^u) C^v}{S_F \text{Tr} \mathcal{P} C^u \text{Tr} \mathcal{P} C^v}$$

546 Example 1

547 This example is the one treated in the main text, where the functions are statistically
 548 independent of one another. Suppose as before that $C^u = C^v = D^2$ ($p = q = 1$) and
 549 $\mathbb{E}F_i = 0$ $\mathbb{E}F_i F_j = \delta_{ij}$ (~~isotropic functions~~) one this condition is what we mean by statistically
 550 independent). One gets that

$$\mathbb{E} \cos^2 \theta_F \simeq \frac{1}{\text{IPR}} + \frac{1}{S_F} - \frac{1}{S_F} \frac{1}{\text{IPR}} = \frac{1}{S_{\text{eff}}}$$

551 so that at first order, the effective dimensionality S_{eff} is the harmonic mean

$$S_{\text{eff}} \approx \frac{1}{\frac{1}{S_F} + \frac{1}{\text{IPR}}}$$

552 as presented in Eq. (8)

553 Example 2

554 ~~Assume~~ For the sake of completeness we treat here the case where the functions are not
 555 statistically independent due to the fact that $m_1 = \mathbb{E}(F_j) \neq 0$ (the average species contributions
 556 to functions tends to be either systematically positive or negative). In this case $\mathcal{P} =$
 557 $m_1^2 P_1 + (m_2 - m_1^2) \mathbb{I}$, where P_1 is a matrix whose elements are all equal to 1, and m_n are the

558 n -th moments of F_i . We have that

$$\begin{aligned}\mathrm{Tr}(\mathcal{P}D^2) &= \mathrm{Tr}(m_1^2 P_1 D^2 + (m_2 - m_1^2) D^2) \\ &= m_2 \|N\|_2^2\end{aligned}$$

559 and so

$$\mathrm{Tr}(\mathcal{P}D^2)^2 = m_1^4 \|N\|_2^4 + (m_2^2 - m_1^4) \|N\|_4^4$$

560 on the other hand, one can show that

$$\mathrm{Tr}\hat{\mathcal{P}}(D^2)D^2 = m_2^2 \|N\|_2^4 + (m_4 - m_2^2) \|N\|_4^4$$

561 if

$$\frac{1}{S_m} = \frac{m_1^4}{m_2^2}$$

562 we get that

$$\frac{(S_F - 1)\mathrm{Tr}(\mathcal{P}D^2)^2}{S_F(\mathrm{Tr}\mathcal{P}D^2)^2} = \frac{1}{S_m} + \frac{1}{\mathrm{IPR}} - \frac{1}{S_m} \frac{1}{\mathrm{IPR}} - \frac{1}{S_F} \frac{1}{S_m} - \frac{1}{S_F} \frac{1}{\mathrm{IPR}} + \frac{1}{S_F} \frac{1}{S_m} \frac{1}{\mathrm{IPR}}$$

563 on the other hand

$$\frac{1}{S_F} \frac{\mathrm{Tr}\hat{\mathcal{P}}(D^2)D^2}{(\mathrm{Tr}\mathcal{P}D^2)^2} = \frac{1}{S_F} - \frac{1}{S_F} \frac{1}{\mathrm{IPR}} + \frac{m_4}{m_2^2} \frac{1}{S_F} \frac{1}{\mathrm{IPR}}$$

564 summing the two gives

$$-\frac{1}{S_m} \frac{1}{\mathrm{IPR}} - \frac{1}{S_F} \frac{1}{S_m} + \left(\frac{m_4}{m_2^2} - 2\right) \frac{1}{S_F} \frac{1}{\mathrm{IPR}} + \frac{1}{S_F} \frac{1}{S_m} \frac{1}{\mathrm{IPR}}$$

565

$$\begin{aligned}\mathbb{E} \cos^2 \theta_F &\approx \frac{1}{S_F} + \frac{1}{S_m} + \frac{1}{\mathrm{IPR}} \\ &\quad - \frac{1}{S_m} \frac{1}{\mathrm{IPR}} - \frac{1}{S_F} \frac{1}{S_m} + \left(\frac{m_4}{m_2^2} - 2\right) \frac{1}{S_F} \frac{1}{\mathrm{IPR}} \\ &\quad + \frac{1}{S_m} \frac{1}{S_F} \frac{1}{\mathrm{IPR}}\end{aligned}$$

566 for a normal distribution

$$m_4 = -2m_1^4 + 3m_2^2$$

567 thus

$$\frac{m_4}{m_2^2} - 2 = 1 - \frac{2}{S_m}$$

568 we then have

$$\begin{aligned}\mathbb{E} \cos^2 \theta_F &\approx \frac{1}{S_F} + \frac{1}{S_m} + \frac{1}{\mathrm{IPR}} \\ &\quad - \frac{1}{S_F} \frac{1}{S_m} - \frac{1}{S_F} \frac{1}{\mathrm{IPR}} - \frac{1}{S_m} \frac{1}{\mathrm{IPR}} - \frac{1}{S_m} \frac{1}{S_F} \frac{1}{\mathrm{IPR}}\end{aligned}$$

569 We see here interactions between the various dimensions S_m , S_F and IPR, with a potential
570 dominance of S_m when all other are much larger. This effective dimensionality emerges due to

571 the collinearity of functions, which thus span a subspace of potentially much smaller dimension
 572 than S_F .

573 S3.3 Change of metric

574 Consider a non euclidean metric tensor H (i.e a positive definite matrix). Distances must now
 575 be measured as

$$\|w\|^2 \rightarrow \langle w|Hw \rangle; \|v\|^2 \rightarrow \langle v|Hv \rangle; \|u\|^2 \rightarrow \langle u|Hu \rangle$$

$$y = \frac{\langle w|Hw \rangle - \langle v|Hv \rangle}{\langle v|Hv \rangle} = \frac{\langle u|Hu \rangle}{\langle v|Hv \rangle} + 2\sqrt{\frac{\langle u|Hu \rangle}{\langle v|Hv \rangle}} \frac{\langle u|Hv \rangle}{\sqrt{\langle v|Hv \rangle \langle u|Hu \rangle}}$$

$$y(x_H) = x_H^2 + 2x_H \frac{\langle u|Hv \rangle}{\sqrt{\langle v|Hv \rangle \langle u|Hu \rangle}}$$

$$\begin{aligned} \mathbb{E}_{u,v} \langle u|Hv \rangle^2 &= \mathbb{E}_{u,v} \langle v|Hu \rangle \langle uH|v \rangle \\ &= \mathbb{E}_v \langle v|HC^u H v \rangle \\ &= \text{Tr} C^v H C^u H \end{aligned}$$

$$\begin{aligned} \mathbb{E}_u \langle u|Hu \rangle &= \mathbb{E}_u \langle u|Hu \rangle \\ &= \text{Tr} C^u H \end{aligned}$$

576 Thus

$$\mathbb{E}_{u,v} \left(\frac{\langle u|Hv \rangle}{\sqrt{\langle v|Hv \rangle \langle u|Hu \rangle}} \right)^2 \approx \frac{\text{Tr} C^v H C^u H}{\text{Tr} C^v H \text{Tr} C^u H} = \frac{1}{S_H}$$

577 the change of metric can thus change the effective dimensionality. In particular, if $C^u \propto C^v \propto \mathbb{I}$
 578 this gives

$$\frac{1}{S_H} = \frac{\sum_{i=1}^S \lambda_i^2}{(\sum_{i=1}^S \lambda_i)^2}$$

579 where λ_i are the eigenvalues of H . Note that H could be the Hessian function (second
 580 derivatives) of a non linear function, computed near the initial state. This explains how
 581 non linear functions can induce a dimensionality effect on the probability of underestimating
 582 change, as illustrated in Fig. S1.

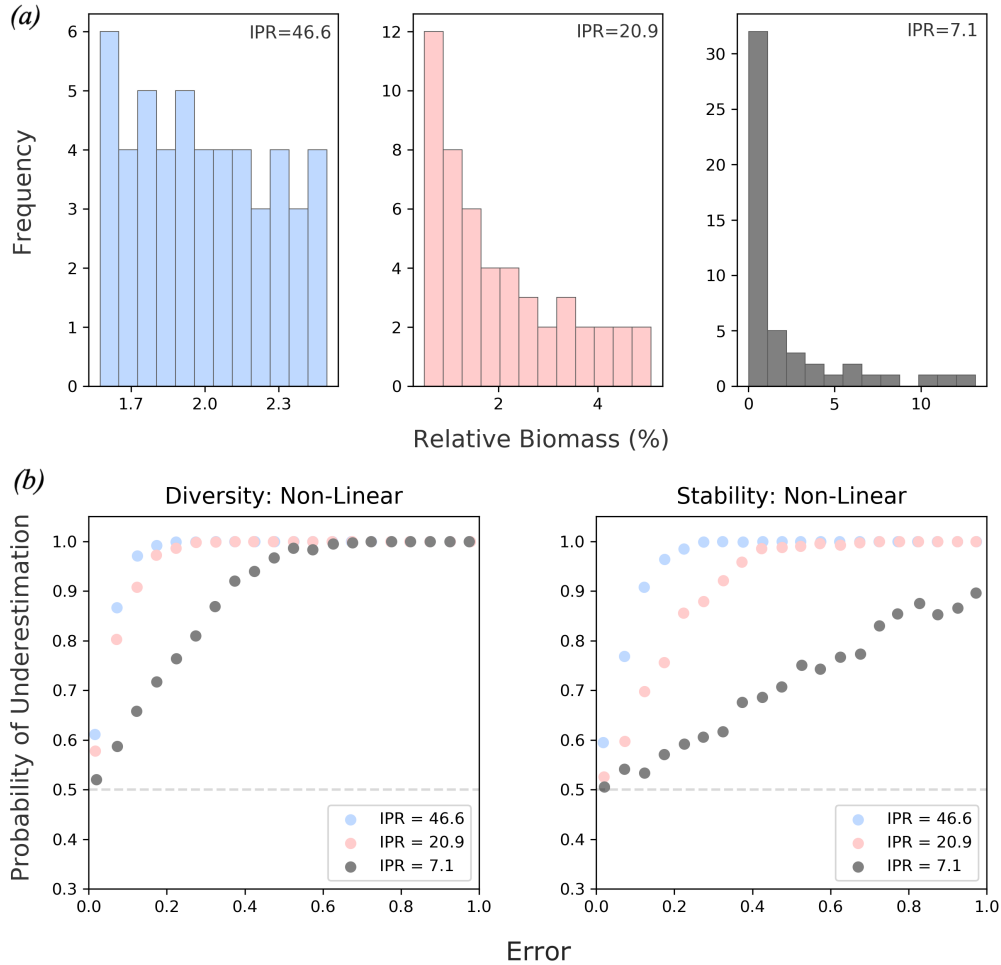


Figure S1: *(a)* Biomass distributions of three 50-species communities with IPR and therefore effective dimensionality of 46.6 (blue), 20.9 (red) and 7.1 (grey). *(a)* The non-linear contribution of diversity (the Shannon index) and stability (invariability) towards the probability of underestimation; it is the non-linear part of a function that is sensitive to the dimensionality of the underlying system.

583 S4 Simulations

584 Initially, the theoretical relationship between error, underestimation and dimensionality was
 585 tested using numerical simulations (Fig. 2(c)). These simulations uniformly sampled the
 586 intersecting circles, spheres and hyper-spheres defined by a prediction of change and relative
 587 error (Fig. 2). This was done for 1-D, 2-D, 10-D and 20-D systems over 10²⁰,000 simulations.
 588 Specifically:

- 589 • a prediction of change and was randomly generated from a normal distribution of mean
 590 0 and standard deviation 1 (defining the blue circle in Fig. 2a).

- 591 • a direction of error was randomly generated from a normal distribution of mean 0 and
592 standard deviation 1, and a magnitude of error was randomly generated from a uniform
593 distribution between 0 and 2 (defining the the red circle in Fig. 2a).
- 594 • From these values, error (x) and underestimation (y) were calculated based on Euclidean
595 distance and subsequently plotted in Fig. 2c).
- 596 • The probability of underestimation $P(y > 0; x)$ was calculated from the simulated results
597 of error and underestimation.

598 As a next step, these simulations were modified to fit ecological problems. In Fig. 1 and Fig. 4
599 the intersecting shapes that are uniformly sampled had dimensions determined by the number
600 of species in a simulated community. However, the dimensions of state space were given
601 unequal weighting of how they respond to change in the form of uneven biomass distributions
602 randomly generated from a log normal distribution of mean 0 and standard deviation 0.05.

603 In Fig. 3 and Fig. S1 communities of 50 species were given unequal biomass distributions by
604 drawing species' biomass from a log scale of varying range; the wider the range of the log
605 scale the more uneven the biomass distribution. Underestimation (y) was calculated using
606 Euclidean distance *and* a number of ecological relevant aggregate properties: the Shannon
607 index (diversity), invariability (stability) and total biomass (functioning).

608 For Fig. 5 our simulations were modified to illustrate that additional dimensional effects
609 come into play when changes in multiple functions are considered at once. Over 50,000
610 simulations 20-D hyper-spheres (community of 20 species) with unequal weighting (IPR of
611 9.9) were uniformly sampled and the results were projected into functional space. Specifically,
612 underestimation was measured for 1, 2, 3, 5 and 10 aggregate functions. [Linear aggregate
613 functions of the form](#)

$$F(B) = \sum_{i=1}^S F_i B_i$$

614 [were defined via the coefficients \$F_i\$, i.e. their sensitivity to the change in the biomass of species
615 \$i\$. The sensitivity of an aggregate function to each species was randomly drawn from a normal
616 distribution of mean 0 and standard deviation 1. This corresponds to the case of statistically
617 independent functions \(see example 1 in subsection S3.2\).](#) State space was then defined by
618 the number of functions.

619 Simulations were conducted in Python with the Matplotlib, NumPy and SciPy libraries. [Code
620 is available in a Jupyter Notebook on GitHub: `https://github.com/jamesaorr/scaling`
621 -up-uncertain-predictions.](#)